



Optics Letters

Utilizing adaptive optics to mitigate intra-modal-group power coupling of graded-index few-mode fiber in a 200-Gbit/s mode-division-multiplexed link

RUNZHOU ZHANG,^{1,*} HAO SONG,¹ HAOQIAN SONG,¹ ZHE ZHAO,¹ GIOVANNI MILIONE,² KAI PANG,¹ JING DU,¹ LONG LI,¹ KAIHENG ZOU,¹ HUIBIN ZHOU,¹ CONG LIU,¹ KARAPET MANUKYAN,¹ NANZHE HU,¹ AHMED ALMAIMAN,^{1,3} JEFFERY STONE,⁴ MING-JUN LI,⁴ BRITTANY LYNN,⁵ ROBERT W. BOYD,⁶ MOSHE TUR,⁷ AND ALAN E. WILLNER¹

¹Department of Electrical Engineering, University of Southern California, Los Angeles, California 90089, USA

²Optical Networking and Sensing Department, NEC Laboratories America, Inc., Princeton, New Jersey 08540, USA

³King Saud University, Riyadh 11362, Saudi Arabia

⁴Corning Incorporated, Sullivan Park, Corning, New York 14831, USA

⁵Space and Naval Warfare Systems Center, Pacific, San Diego, California 92152, USA

⁶The Institute of Optics, University of Rochester, Rochester, New York 14627, USA

⁷School of Electrical Engineering, Tel Aviv University, Ramat Aviv 69978, Israel

*Corresponding author: runzhou@usc.edu

Received 3 April 2020; revised 15 May 2020; accepted 20 May 2020; posted 20 May 2020 (Doc. ID 394307); published 25 June 2020

We experimentally demonstrate the utilization of adaptive optics (AO) to mitigate intra-group power coupling among linearly polarized (LP) modes in a graded-index few-mode fiber (GI FMF). Generally, in this fiber, the coupling between degenerate modes inside a modal group tends to be stronger than between modes belonging to different groups. In our approach, the coupling inside the LP₁₁ group can be represented by a combination of orbital-angular-momentum (OAM) modes, such that reducing power coupling in OAM set tends to indicate the capability to reduce the coupling inside the LP₁₁ group. We employ two output OAM modes $l = +1$ and $l = -1$ as resultant linear combinations of degenerate LP_{11a} and LP_{11b} modes inside the LP₁₁ group of a ~ 0.6 -km GI FMF. The power coupling is mitigated by shaping the amplitude and phase of the distorted OAM modes. Each OAM mode carries an independent 20-, 40-, or 100-Gbit/s quadrature-phase-shift-keying data stream. We measure the transmission matrix (TM) in the OAM basis within LP₁₁ group, which is a subset of the full LP TM of the FMF-based system. An inverse TM is subsequently implemented before the receiver by a spatial light modulator to mitigate the intra-modal-group power coupling. With AO mitigation, the experimental results for $l = +1$ and $l = -1$ modes show, respectively, that (i) intra-modal-group crosstalk is reduced by > 5.8 dB and > 5.6 dB and (ii) near-error-free bit-error-rate performance is achieved with a penalty of ~ 0.6 dB and ~ 3.8 dB, respectively. © 2020 Optical Society of America

<https://doi.org/10.1364/OL.394307>

There has been much interest in utilizing space-division-multiplexing (SDM) as a technique to further increase capacity in optical communication systems [1]. A subset of SDM is the transmission of multiple orthogonal spatial modes in a few mode fiber (FMF) to achieve mode-division multiplexing (MDM) [2]. Typically, an FMF can accommodate a limited set of linearly polarized (LP) modes such that each mode carries an independent data channel [3,4].

During propagation along the FMF, LP modes tend to experience modal power coupling and inter-channel crosstalk (XT) [5]. Moreover, the supported modes of an FMF can be degenerate (e.g., two-fold degenerate LP_{11a} and LP_{11b} modes) and divided into different groups. Different modes from different modal groups (e.g., LP₀₁, LP₁₁, and LP₂₁) tend to be weakly coupled because of the larger difference in their group velocities. Conversely, different modes in the same degenerate group would tend to experience stronger power coupling and XT since they share a similar group velocity [6].

In the case of weaker power coupling among modal groups, an MDM system using FMF can still operate if each independent data stream is (i) transmitted on a different modal group, (ii) transmitted on only one mode within that group, and (iii) recovered by detecting only the modes within that group having strong coupling [7,8]. Alternatively, approaches to mitigate this weak inter-group power coupling include (i) recover multiple signals simultaneously from multiple modes and apply electronic multiple-input-multiple-output (MIMO) equalization algorithms [3,4], and (ii) measure the distortion of each mode after FMF propagation and then correct the distortion by using an optical spatial light modulator (SLM). Such an “optical

equalization,” called digital optical phase conjugation (DOPC), tends to enable the accommodation of high-bandwidth data channels [9].

With respect to the stronger XT inside modal groups, one approach to limit such XT is to use a specially designed fiber, such as an elliptical-core FMF [10,11]. However, for a circular-graded-index (GI)-FMF-based MDM transmission, electronic MIMO processing is typically used for mitigating the XT and recovering the multiplexed channels within a degenerate group [3,4,12].

In this Letter, we experimentally demonstrate the utilization of adaptive optics (AO) to optically mitigate intra-modal-group strong power coupling in a GI FMF. In our approach, the stronger coupling inside the LP₁₁ group can be inferred from the resultant linear combinations of output OAM $l = +1$ and $l = -1$ modes [13,14]. Each OAM mode carries a quadrature-phase-shift-keying (QPSK) signal at data rates 20, 40, or 100 Gbit/s, propagating through a ~ 0.6 -km GI FMF. We first measure the transmission matrix (TM), which represents power coupling within the LP₁₁ group. Subsequently, we apply the AO approach to implement the inverse TM to the coupled modes in order to mitigate XT. With AO mitigation, the experimental results for OAM $l = +1$ and $l = -1$ modes show, respectively, that: (1) modal XT are reduced from -8.4 dB and -4.6 dB to -14.3 dB and -10.2 dB, if both modes carry a 50-Gbaud QPSK signal, and (2) bit-error rate (BER) values for both data channels are achieved below the 7% forward error correction (FEC) limit with optical signal-to-noise ratio (OSNR) penalties of approximately 0.9 dB and 3 dB, 1 dB and 1.8 dB, and 0.6 dB and 3.8 dB for 10-Gbaud, 20-Gbaud, and 50-Gbaud QPSK signals, respectively.

Generally, in addition to LP mode, OAM mode can also be used as a modal-basis tool to characterize and control the modal power coupling in a GI FMF [15]. This is due to the fact that LP modes can be represented by linear combinations of OAM modes [13]. As shown in Fig. 1(a), for the LP₀₁ and LP₁₁ modal groups of a GI FMF, the power coupling between degenerate LP_{11a} and LP_{11b} modes tends to be stronger than the coupling between LP₀₁ and LP_{11a} (or LP_{11b}) modes. In this demonstration, such strong coupling within the LP₁₁ group

would correspond to modal XT between output OAM $l = +1$ and $l = -1$ modes. Moreover, if an approach can mitigate modal power coupling in the OAM basis, it tends to indicate the capability to mitigate coupling between the corresponding LP modes [13,15,16].

The concept of using AO to mitigate intra-group modal XT is shown in Fig. 1(b). Two independent data channels are transmitted inside the LP₁₁ group, and the power of the transmitted channels would couple to each other during their propagation inside the FMF. As a result of the intra-group modal coupling, the output data channels would contain both the LP_{11a} and LP_{11b} component. We can also describe such modal coupling as a complex 2×2 matrix M at the basis of OAM $l = +1$ and $l = -1$. The amplitude and phase of complex elements in matrix M are related to the power coupling and phase delay between the two OAM modes, respectively. AO then applies an inverse matrix S to the mixed signals [17]:

$$S = M^{-1} = \begin{bmatrix} s_{11} & s_{12} \\ s_{21} & s_{22} \end{bmatrix} = \begin{bmatrix} \mathbf{s}_1^T \\ \mathbf{s}_2^T \end{bmatrix},$$

where $\mathbf{s}_1^T = [s_{11} \ s_{12}]$ and $\mathbf{s}_2^T = [s_{21} \ s_{22}]$ are the row vectors of matrix S and all elements of S are complex numbers. The phase mask for the AO mitigation is constructed by using a complex combination of OAM $l = +1$ and $l = -1$ demultiplexing phase patterns, the weights of which are given by \mathbf{s}_1^T (\mathbf{s}_2^T) for mitigating the $l = +1$ ($l = -1$) data channel. Such a phase mask converts the two OAM modes to Gaussian beams simultaneously with the designed complex conversion efficiencies (i.e., either \mathbf{s}_1^T or \mathbf{s}_2^T), and the XT component in the received signal would have little power coupled into the coherent signal detection.

The experimental setup is shown in Fig. 2(a). At the transmitter (Tx), an up-to-100-Gbit/s QPSK data stream is generated at ~ 1.55 μm by an in-phase-quadrature (IQ) modulator. It is then amplified and sent into a 50/50 fiber coupler. One of the two copies is delayed by a ~ 1 -m single-mode fiber (SMF) to decorrelate the data sequences, and both copies are sent to an OAM mode multiplexer (CAILabs, [18]) to generate coaxial $l = +1$ and $l = -1$ modes in free space. An OAM mode is described by its azimuthal index l , referring to the number of 2π phase shifts along the azimuthal direction on its phase front [19]. The polarizations of these two data-carrying OAM modes are adjusted by two fiber-based polarization controllers and then a free-space polarizer ensures that they have the same polarization. An objective lens (20 \times) is used to couple the modes into a ~ 0.6 -km GI FMF, which supports the LP₀₁, LP₁₁, LP₂₁, and LP₀₂ degenerate modal groups. After propagation in the FMF, the output modes are coupled back to the free space by a collimator. The OAM multiplexer induces a ~ 2.2 dB and ~ 3.5 dB power loss for OAM $l = +1$ and $l = -1$ modes, respectively. Moreover, the free-space-to-FMF coupling at the Tx together with the FMF propagation induces a ~ 7.6 dB and ~ 7.3 dB power loss to the OAM $l = +1$ and $l = -1$ modes, respectively. The intensity profiles of the FMF input and the corresponding output modes are also shown in Fig. 2(a). The input modes are donut-shaped $l = +1$ and $l = -1$ modes with little power in the beam center; the output modes are observed to contain two intensity lobes, which are combinations of LP₁₁ modes. This is consistent with the fact that OAM and LP modes can be represented by linear superpositions of each other [13]. At the receiver (Rx), the polarizations of output modes are tuned

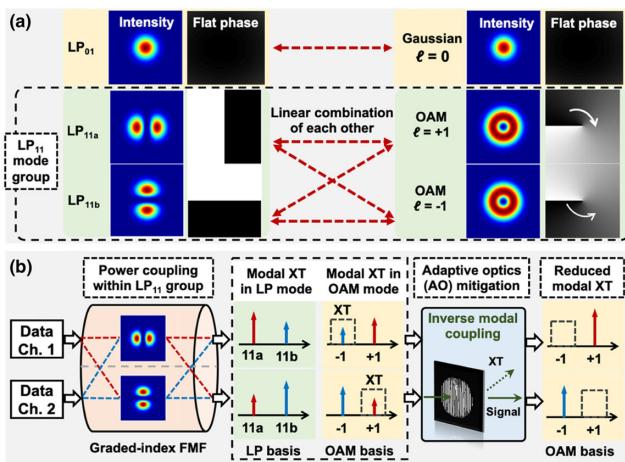


Fig. 1. (a) Relationship examples between LP and OAM modes. (b) Concept diagram for AO to mitigate modal XT inside the LP₁₁ group of a GI FMF: AO implements an inverse TM to the coupled output modes.

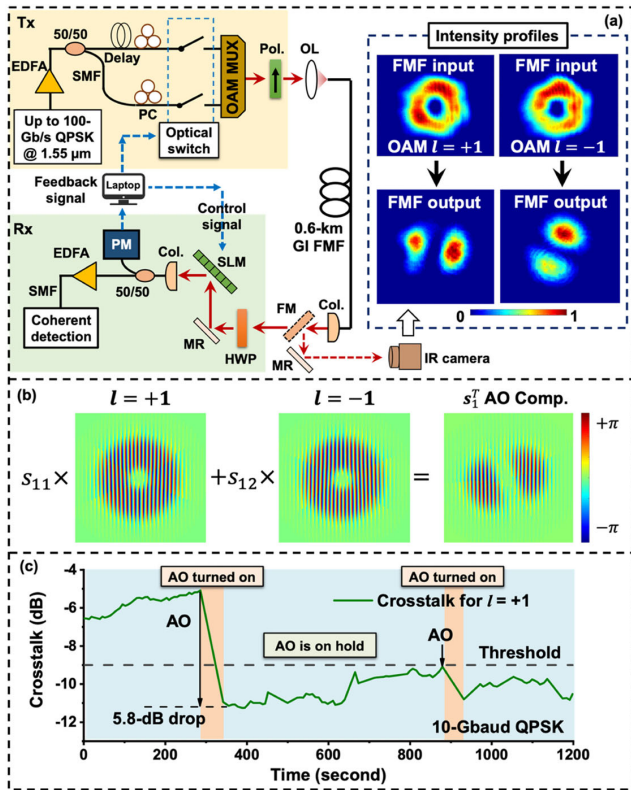


Fig. 2. (a) Experimental setup for AO to mitigate modal XT in FMF-based MDM system. EDFA: erbium-doped fiber amplifier; PC: polarization controller; MUX: multiplexer; Pol.: polarizer; Col.: collimator; FM: flip mirror; MR: mirror; IR: infrared; PM: power monitor. (b) An example of AO phase mask to mitigate data channel 1 carried by OAM $l = +1$. (c) Measured time-varying XT for the OAM $l = +1$ mode.

by a half-wave plate (HWP) to be aligned with the polarization of the polarization-sensitive SLM. After being spatially transformed by the SLM, the reflected light beams are coupled into an SMF and then equally split to two copies. One copy is sent for coherent signal detection and the other copy is sent for TM measurement. Our AO approach induces a power loss of up to ~ 5.5 dB to the mitigated mode, i.e., either $l = +1$ or $l = -1$. Additionally, the free-space-to-SMF coupling at the Rx is ~ 4 dB in this demonstration. We note that when more modes (>2) are multiplexed in the system, only one coupler is required to split power and enable the TM measurement. We also note that the $1/N$ insertion loss for mode demultiplexing may be reduced by using a low-loss mode demultiplexer, such as by using multi-plane light conversion [18].

The process of AO mitigation includes the following three steps. Step 1: Measure the complex 2×2 TM (i.e., matrix M) of the FMF using the method in Refs. [17,20]. To measure both the amplitude and phase of each element of the TM, we transmit one data-carrying mode at a time from the Tx and correspondingly load different phase masks on the SLM at the Rx. The amplitude of each element is obtained by direct power measurement when the SLM is loaded with either the OAM $l = +1$ or $l = -1$ individual demultiplexing pattern. The phase of each element is calculated from the four power measurements

obtained when the SLM is sequentially loaded with four different phase masks. These masks are the combinations of $l = +1$ and $l = -1$ individual demultiplexing patterns with $0, \pi/2, \pi,$ and $3\pi/2$ phase delays. Step 2: Calculate the inverse matrix of M using $S = M^{-1}$, where S is also a 2×2 complex matrix. The two rows of coefficients $[s_{11} \ s_{12}]$ and $[s_{21} \ s_{22}]$ are used to mitigate the XT for the data channels carried by the OAM $l = +1$ and $l = -1$ modes, respectively. Step 3: Construct a mitigation phase mask by combining the OAM $l = +1$ and $l = -1$ demultiplexing phase patterns, the weights of which are given by s_{11} and s_{12} for data channel 1 and s_{21} and s_{22} for data channel 2, respectively. Figure 2(b) shows an example of the AO mitigation phase mask for the data channel 1.

As shown in Fig. 2(c), we take ~ 120 XT measurements from 0 to 1200 s. At each measurement, we determine the modal XT by alternately transmitting the OAM $l = +1$ and then the $l = -1$ mode from the Tx, and subsequently detecting the ratio of power coupling to the non-transmitted mode at the Rx. The XT fluctuates from -7 dB to -5 dB for the first ~ 300 s since no AO is applied; the XT drops by >5.8 dB to <-11 dB when we apply the AO to mitigate modal power coupling. From ~ 300 to ~ 880 s, the mitigation phase pattern is kept fixed; subsequently, the XT varies and the mitigation degrades over time. To re-suppress the XT, we manually set a threshold of ~ -9 dB and would repeat the AO as the XT reaches the threshold. For example, the XT drops again after we refresh the AO at ~ 880 s. In our demonstration, we manually adjust the transmission of different modes (i.e., AO switching time) based on Rx measurements, which produces a slow AO mitigation of ~ 50 s. However, this could be automated with an electronic feedback loop and produce significantly shorter AO mitigation response times as limited by the SLM refresh rate [10].

We then utilize the AO mitigation to a two-channel 200-Gbit/s MDM link, with each OAM mode carrying an independent 100-Gbit/s QPSK data stream. As shown in Fig. 3(a), the measured XT for $l = +1$ and $l = -1$ mode is decreased from -8.4 dB and -4.6 dB to -14.3 dB and -10.2 dB, and the error vector magnitude (EVM) is dropped from 62.2% and 60.6% to 22.1% and 25.6%, respectively. Without AO mitigation, the coherent detection algorithm in this demonstration does not readily recover the I-Q information of both the data channels because of the high XT, which produces an EVM value of $>60\%$. With the AO approach, the

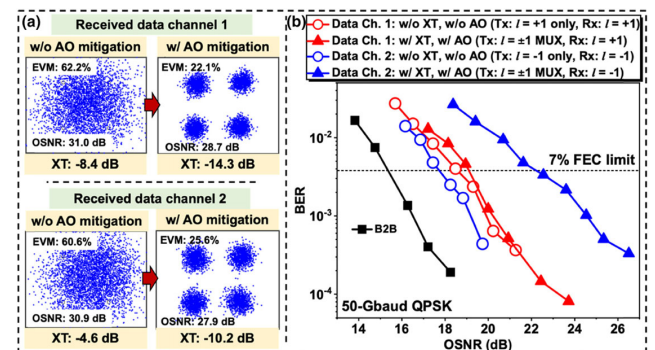


Fig. 3. Measured BER performance for multiplexed data channel 1 and 2 with and without AO mitigation: (a) Constellations for QPSK signal. (b) BER versus OSNR. Data channels are 100-Gbit/s QPSK signals.

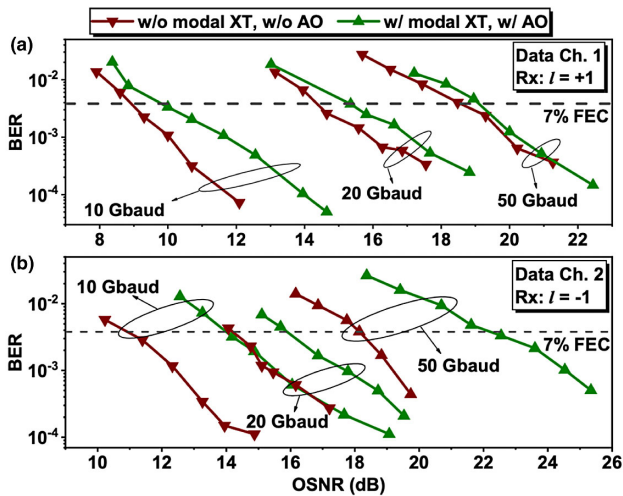


Fig. 4. BER performance with AO mitigation for different data rates (10-, 20-, and 50-Gbaud QPSK): (a) data channel 1 carried by OAM $l = +1$ mode; (b) data channel 2 carried by $l = -1$ mode.

XT is reduced by ~ 5.6 dB for data channel 2 (carried by the $l = -1$ mode), thus helping to enable the algorithm to recover the I-Q information with a lower EVM of $\sim 25.6\%$. As shown in Fig. 3(b), for comparison, we first measure the BER performance of transmitting a single 100-Gbit/s QPSK data channel carried by $l = +1$ or $l = -1$ mode without AO mitigation: a ~ 3.1 dB and ~ 2.1 dB OSNR penalty are observed at the 7% FEC limit, respectively. We then measure the BER performance for these two data channels when they are transmitted simultaneously. After AO mitigation, these two channels carried by $l = +1$ and $l = -1$ mode can achieve BER under the 3.8×10^{-3} FEC limit, and the OSNR penalties are ~ 0.6 dB and ~ 3.8 dB larger than that of the BER performance for transmitting the corresponding single channels, respectively. The AO achieves a XT of -10.2 dB for $l = -1$ mode as compared with -14.3 dB for $l = +1$ mode. This may be attributed to the fact that the specific OAM multiplexer used in our demonstration couples the $l = -1$ mode into the LP₁₁ group with lower efficiency, thus limiting the corresponding data channel's signal power collected by the AO. We note that the AO-mitigated XT for the $l = -1$ mode could be reduced by optimizing the coupling efficiency and OAM modal purity at the FMF input [4].

We also apply the AO mitigation to multiplexed data channels with different data rates. As shown in Fig. 4, the AO can reduce XT and achieve a BER below the 7% FEC limit for transmitting both modes carrying 10-, 20-, and 50-Gbaud QPSK signals. With the AO mitigation, the OSNR penalty at the FEC limit for $l = +1$ and $l = -1$ mode is measured as ~ 0.9 dB and ~ 3 dB for the 10-Gbaud signal and ~ 1 dB and ~ 1.8 dB for the 20-Gbaud signal, respectively.

To mitigate modal power coupling, the complex TM of the FMF is measured by adaptively switching the transmitted OAM modes. By designing training sequences for both data channels, the requirement for the feedback between the Tx and Rx may be reduced [9]. In order to multiplex more modes (> 2) in an FMF, we note that several limiting factors should be considered: (i) lower loss mode (de)multiplexing [18] and (ii) effective com-

ensation of chromatic dispersion and modal differential group delays [21].

Funding. Vannevar Bush Faculty Fellowship sponsored by the Basic Research Office of the Assistant Secretary of Defense (ASD) for Research and Engineering (RE) and funded by the Office of Naval Research (N00014-16-1-2813); National Science Foundation (ECCS-1509965).

Disclosures. The authors declare no conflicts of interest.

REFERENCES

- D. J. Richardson, J. M. Fini, and L. E. Nelson, *Nat. Photonics* **7**, 354 (2013).
- P. Sillard, *Optical Fiber Communication Conference* (Optical Society of America, 2016), paper Th1J.1.
- R. Ryf, S. Randel, A. H. Gnauck, C. Bolle, A. Sierra, S. Mumtaz, M. Esmaelpour, E. C. Burrows, R. J. Essiambre, P. J. Winzer, D. W. Peckham, A. H. McCurdy, and R. Lingle, *J. Lightwave Technol.* **30**, 521 (2012).
- S. Randel, R. Ryf, A. Sierra, P. J. Winzer, A. H. Gnauck, C. A. Bolle, R.-J. Essiambre, D. W. Peckham, A. McCurdy, and R. Lingle, *Opt. Express* **19**, 16697 (2011).
- K. Kitayama and N. Diamantopoulos, *IEEE Commun. Mag.* **55**(8), 163 (2017).
- J. Carpenter, B. C. Thomsen, and T. D. Wilkinson, *J. Lightwave Technol.* **30**, 3946 (2012).
- T. Hu, J. Li, D. Ge, Z. Wu, Y. Tian, L. Shen, Y. Liu, S. Chen, Z. Li, Y. He, and Z. Chen, *Opt. Express* **26**, 8356 (2018).
- K. Benyahya, C. Simonneau, A. Ghazisaeidi, R. R. Muller, M. Bigot, P. Sillard, P. Jian, G. Labroille, J. Renaudier, and G. Charlet, *European Conference on Optical Communication (ECOC)* (2018), paper Tu1G.5.
- S. Bae, Y. Jung, B. G. Kim, and Y. C. Chung, *IEEE Photon. Technol. Lett.* **31**, 739 (2019).
- E. Ip, G. Milione, M.-J. Li, N. Cvijetic, K. Kanonakis, J. Stone, G. Peng, X. Prieto, C. Montero, V. Moreno, and J. Liñares, *Opt. Express* **23**, 17120 (2015).
- G. Milione, E. Ip, M.-J. Li, J. Stone, G. Peng, and T. Wang, *Opt. Lett.* **41**, 2755 (2016).
- H. Takahashi, D. Soma, S. Beppu, and T. Tsuritani, *IEEE Photonics Conference (IPC)* (2019), paper ThB1.1.
- H. Huang, G. Milione, M. P. J. Lavery, G. Xie, Y. Ren, Y. Cao, N. Ahmed, T. A. Nguyen, D. A. Nolan, M.-J. Li, M. Tur, R. R. Alfano, and A. E. Willner, *Sci. Rep.* **5**, 14931 (2015).
- R. Zhang, H. Song, H. Song, Z. Zhao, K. Pang, J. Du, G. Labroille, C. Liu, H. Zhou, K. Manukyan, M. Tur, and A. Willner, *European Conference on Optical Communication (ECOC)* (2019), paper W.3.C.2.
- S. Chen and J. Wang, *Sci. Rep.* **7**, 3990 (2017).
- J. Carpenter, B. J. Eggleton, and J. Schröder, *Opt. Express* **22**, 96 (2014).
- H. Song, H. Song, R. Zhang, K. Manukyan, L. Li, Z. Zhao, K. Pang, C. Liu, A. Almairan, R. Bock, B. Lynn, M. Tur, and A. E. Willner, *J. Lightwave Technol.* **38**, 82 (2020).
- G. Labroille, B. Denolle, P. Jian, P. Genevaux, N. Treps, and J.-F. Morizur, *Opt. Express* **22**, 15599 (2014).
- A. M. Yao and M. J. Padgett, *Adv. Opt. Photon.* **3**, 161 (2011).
- G. Xie, H. Song, Z. Zhao, G. Milione, Y. Ren, C. Liu, R. Zhang, C. Bao, L. Li, Z. Wang, K. Pang, D. Starodubov, B. Lynn, M. Tur, and A. E. Willner, *Opt. Lett.* **42**, 4482 (2017).
- R. Ryf, M. A. Mestre, S. Randel, C. Schmidt, A. H. Gnauck, R. J. Essiambre, P. J. Winzer, R. Delbue, P. Pupalakis, A. Sureka, Y. Sun, X. Jiang, D. W. Peckham, A. McCurdy, and R. Lingle, *IEEE Photon. Technol. Lett.* **24**, 1965 (2012).